EFFECTS OF EARTHQUAKES ON UNDERWATER STRUCTURES

Ray W. Clough[1]

INTRODUCTION

It has been known for many years that objects immersed in or in contact with a fluid exhibit different dynamic properties than are observed for the same objects in air. Early experiments, dating back as far as the work of P. L. G. Dubaat late in the 18th century, demonstrated that the motions of the fluid in contact with the dynamic system give rise to an effect which is equivalent to an increase in the apparent mass of the system.

The hydrodynamic equations required to evaluate this added mass effect for any given system are too complex to be discussed here. However, an explanation of the phenomenon based on energy principles provides some insight into its physical significance and may be presented quite simply.

In general, the effective mass, M, of any dynamic system may be related to its kinetic energy of motion, T, by the familiar expression

$$T = \frac{1}{2} M v^2 \tag{1}$$

in which v is the velocity of some representative point in the system. When the same system is in contact with a fluid, however, the motion of the system causes the surrounding fluid itself to move in some related fashion. The fluid thus possesses kinetic energy, T_a, which can also be expressed in terms of the velocity of the dynamic system, v; thus

$$T_a = \frac{1}{2} M_a v^2 \tag{2}$$

The quantity M_a, in this expression, is a constant relating the kinetic energy of the fluid to the velocity of the dynamic system. It has the dimensions of mass and generally is termed the "added mass" of the fluid. Its value depends upon the shape and size of the dynamical system, the type of motion to which it is subjected, and the mass density of the surrounding fluid.

---

1. Professor of Civil Engineering, University of California, Berkeley.

It will be noted now that the total kinetic energy, T_v, of the dynamic system and fluid may be written

$$T_v = \frac{1}{2}(M + M_a)v^2 = \frac{1}{2} M_v v^2 \qquad (3)$$

Here, M_v represents the effective mass of the dynamic system plus the added mass of the surrounding fluid, and is called the "virtual mass". The virtual mass of a system in contact with a fluid plays the same role in dynamic analyses as does the effective mass of the system in air; it controls both the vibration frequencies and the dynamic forces which are developed. (Strictly speaking, the added mass effect should be considered even for structures in air, but the added mass of the air is a negligible factor except in special cases such as airplane wing vibrations).

Because of its importance in problems of structural dynamics, the magnitude of the added mass to be associated with various types of structures in contact with water has been the subject of many investigations over a span of many years. Naval architects have studied the problem in connection with both rigid body and elastic motions of ship hulls (1)[1]; harbor engineers have been concerned with related effects associated with wave forces on structures (2); civil engineers have made limited studies of added mass effects in the earthquake response of underwater structures (3,4); and hydrodynamicists have explored the subject as a problem in the theory of fluid mechanics (5). For limited ranges of conditions, for example for rigid spheres or circular cylinders subjected to small amplitude harmonic motions, these investigations have led to adequate estimates of the added mass. However, there is considerable doubt that these results may be applied indiscriminately to the earthquake response of structures under water. In such a case, the structure may have a form quite different from the simple shapes previously studied; it probably will undergo significant amounts of flexural deformation, and the motion to which it is subjected certainly is anything but simple harmonic.

It was to provide some quantitative information regarding the added mass values appropriate to the evaluation of the earthquake response of underwater structures that the present study was undertaken. The specific objectives of the study were to determine added mass values pertinent to simple, prismatic forms of structures considering the effects of

1) Irregular, earthquake-like ground motions, and

2) Flexural deformations of the structure.

A third objective had been considered at the time the project was initiated: evaluation of the magnitude of ground motions required to cause a transition in flow characteristics from the type characteristically associated with structural vibrations (6) to the conditions pertaining to wave action on structures (7). However, it appears that this latter condition is not likely to develop in earthquake motions; and

---

1. Numbers in parentheses refer to similarly numbered items in the Bibliography.

because this phase of the work would require ground motions exceeding the capabilities of the test equipment, it was not included in the present study.

EXPERIMENTAL EQUIPMENT

The results reported in this paper were obtained by model tests, using the shaking table of the University of California Structural Engineering Laboratory to produce the model earthquakes, and mounting models of the desired forms on the table in a tank of water supported over the table. Details of the test apparatus, models, and instrumentation are discussed below.

Shaking Table

The shaking table used in this study consists of a 7 ft by 10 ft reinforced concrete slab, 8 inches thick, mounted on flexible legs which permit it one degree of freedom of motion, and excited by a 140 lb pendulum striking a buffer spring. Details of its construction have been reported previously (8) and will not be repeated here. To provide the fluid medium surrounding the models studied in this test, a set of plywood walls extending to a height of 28 inches above the table top were erected on steel supports attached to the floor and independent of the table. A flexible rubber membrane was used to seal the small space between the table top and the walls, thus allowing free motion of the table with respect to the stationary body of water resting on it. The shaking table, with tank walls in place, is shown in Fig. 1.

Models

Two series of models were tested during this investigation. The first consisted of rigid prismatic aluminum members mounted in a horizontal position on flexible legs, with the axis of the member perpendicular to the direction of table motion. The table motion excited a single mode of vibrational response of the models: translation along the table axis (transverse to the model axis). Four different natural frequencies of vibrational response were obtained for each model by using legs with free lengths of 7, 10, 13, and 16 inches in successive tests. The models were attached to the flexible legs by means of rigid end plates designed to restrict fluid flow about the ends of the cylinders, thus creating essentially two-dimensional flow conditions over the entire length of the model. Five different cross-sectional shapes were tested, as follows: 1.5 in. and 3 in. diameter hollow circular sections, 3 in. by 3 in. and 3 in. by 1.75 in. hollow rectangular sections, and a 3 in. by 3/8 in. solid plate section. The rectangular sections were all tested with the 3 in. dimension facing in the direction of motion. The complete set of horizontal models, one mounted on its flexible legs, is shown in Fig. 2.

The second series of models consisted of vertical cantilever columns of the same cross-sectional shapes as the horizontal models (excluding the 1.5 in. diameter circular section), and 24 in. in height. To maintain the desired cross-sectional shapes, and at the same time permit a significant degree of flexibility, these models were built up by attaching rigid segments of aluminum tubing of appropriate shape to a 1/4 in. by 1 in.

aluminum beam. The 2 7/8 in. long segments were attached at a spacing of 3 in. on centers, thus requiring 8 segments for the 24 inch height. The 1/8 inch spaces between segments were covered with thin rubber membranes to prevent flow of water between them, and the top end was similarly closed. In one test series on the flat plate cross-section, a 4.92 lb weight was attached rigidly with its center of gravity 2 inches above the top of the column (i.e. above the water surface). This caused a significant change in the vibrational mode shape and frequency of the model, and simulated a structure, such as a bridge pier, supporting a system above water. The segmented vertical model with part of the square section tubular segments attached is shown in Fig. 3, together with a typical segment of each of the other sections studied, and the extra weight which could be attached at the top of the flat plate model.

Instrumentation

Instrumentation was required in the test program to record both the motion of the shaking table and the response of the models. The shaking table motion was recorded only during a preliminary test series because it soon became evident that the table motion was not affected by the response of any of the models considered during the test program. Thus it was possible to record a "standard" table motion, and apply it in all of the test cases. The table instrumentation consisted of a Statham accelerometer and a clip gage, the latter being used to record displacements. Both transducers operated on the resistance wire principle, and their output was recorded on a Sanborn direct-writing oscillograph. A record of the standard table accelerations is shown in Fig. 4.

The response of the models of Series I was measured by a Statham accelerometer mounted internally at the center of the hollow cylindrical sections (or attached externally to the flat plate model). The accelerometer output was recorded by a Sanborn recorder, with typical records appearing as shown in Fig. 5.

Measuring the response of the vertical cantilever model was a more complex problem because of its multiple degrees of freedom. It was decided that the most significant measure of its response was the time variation of bending moments at various levels in its height. To measure these, resistance wire strain gages were mounted in pairs at four levels: one-half inch, and 6, 12, and 18 inches above the base. These gages were connected so as to measure bending strains directly, and their output was recorded on a four-channel Sanborn recorder. Typical records from such a test are shown in Fig. 6.

THE SIMULATED EARTHQUAKE

As was noted above, the simulated earthquake motion caused by the impact of the pendulum against the buffer spring was standardized, and the same motion was used for all tests. That this motion is not an exact replica of the chaotic, random accelerations of a real earthquake is evident from the record shown in Fig. 4. The table accelerations, although somewhat irregular during the initial contact phase, are largely simple harmonic in form.

In order to determine the suitability of this simulated earthquake for test purposes, a digital computer analysis was made of the acceleration response spectrum developed by the early phases of the motion. Input data was evaluated from the enlarged reproduction of the table acceleration record shown in Fig. 7a, and the undamped acceleration response spectrum calculated for five different durations of 'quake motion, as indicated. The calculated results are shown in Fig. 7b. These curves show that shortening the earthquake duration has the effect of removing the resonant response peak associated with the natural frequency of the table. While such a peak might be representative of earthquakes in a region where there is a predominate vibration period of the ground motion, for the general case, a flatter response spectrum seems more realistic. Consequently the 0.191 second duration was selected as the standard earthquake. This means that only the first 0.191 seconds was considered in the model response records obtained during the test program.

Effects of size reduction also may be important in model tests such as these, and it is of interest to consider what scale effects might be anticipated. One factor which may contribute to scale effects in any hydrodynamic test is the viscous drag force of the fluid. When the same fluid is used in both model and prototype tests, it is impracticable to maintain both viscous and inertia forces in the same scale ratio between model and prototype. For example, using a model length scale of 1/10, the model accelerations would have to be 1000 times those in the prototype to keep the drag forces in scale. Thus the model equivalent of a 1/10g earthquake would require test accelerations up to 100g, which is manifestly impossible with the equipment used in this program.

Because this difficulty is inherent in any hydrodynamic model tests, the Reynold's Number (which represents the ratio between inertia and viscous forces) has become important as a measure of the significance of the viscous forces: where the Reynold's number is high, viscosity effects can be neglected with little error. For the type of system described in this paper, the Reynold's number for the prototype is on the order of 10^6, while in the model it is on the order of 10^4, indicating that while viscosity effects are small in both cases, they are much more important in the model than in the prototype. However, since vibration tests of the models demonstrated very low damping effects, it may be concluded that this lack of similitude is of no great importance.

Another scale factor which might be noted here is the ratio of the table displacements to the model dimensions. This ratio was on the order of 1/40 which if carried over to the prototype would require that a 3 inch earthquake displacement be related to a prototype structure with a cross-sectional dimension on the order of 10 feet. It is to this class of structure that these studies may be considered directly applicable. For much smaller cross-sections (on the order of a few inches in the prototype), flow conditions similar to those resulting from wave action against structures might become a factor in the earthquake response.

TEST PROCEDURE AND RESULTS

Series I

The objective of the first test series, using the horizontal models, was to evaluate the added mass associated with rigid prismatic bodies of various cross-sectional shapes when subjected to a simulated earthquake motion. This was accomplished by observing the response to the standard table motion of each of the models under water, and then experimentally determining the mass which had to be added in each case to obtain the same response in air. This mass, which was added in the form of steel pieces rigidly clamped to the model, was a direct representation of the added mass of the water. It was not possible to obtain records which were completely identical to the underwater records this way, because damping conditions were not the same. However, very similar records were obtained during the early phases of the table motions, and this was the only part of the record of interest to this investigation. Records of the model response under water, in air with no added mass, and in air with the experimentally determined added mass for a typical case are shown in Fig. 5. Values of the weights added to the models for each case, to give results in air equivalent to those observed in water, are summarized in the third column of Table I.

As a second phase of Test Series I, the added mass values associated with simple harmonic vibratory motions of the models were evaluated from observations of the frequency of free vibrations of the models under water. Records of free vibrations were obtained by releasing the models from a displaced position, and from the observed frequencies of vibration and from the measured stiffnesses of the various sets of legs, it was possible to compute the virtual mass of the model. Values of the added masses obtained in this way are summarized in the fourth column of Table I. These represent averages of the values obtained with the four different sets of legs used with each model. Also presented in Table I are the added mass coefficients obtained by the earthquake test and by the free vibration test. These coefficients represent the ratio of the experimentally determined added weight to the weight of water displaced by a right circular cylinder with a diameter equal to the maximum transverse dimension of the model, and are fundamental properties of the various shapes considered. As a matter of interest, damping ratios evaluated from free vibration records obtained in air and under water with the various models are presented in Table II. These values represent averages of the ratios obtained in the four cases studied for each model (four leg lengths).

Another type of result obtained from the earthquake tests of the Model Series I is presented in Fig. 8. This shows the maximum acceleration observed for each test (within the 0.191 second duration of the standard earthquake) plotted as a function of the period of vibration of the model. Thus this graph, by definition, is the experimentally determined acceleration spectrum of the earthquake motion. Two different curves have been drawn through the data points, one for the models tested in air, and the other for models under water; and a definite reduction of response is apparent for the models in water. Acceleration spectra obtained by digital computer analysis of the table motions for 0 and 2% damping are presented as dotted lines for comparison.

Series II

It wasn't practical to attempt to determine added mass values for the vertical models of Test Series II by the techniques used in the first series because of the complexity of the response of these multi-degree of freedom systems, and also because the mass could be distributed in an infinite variety of patterns. Instead, the period of the fundamental mode of vibration of each model in water was measured, and then uniformly distributed mass was added to produce the same fundamental period in air. Periods of the second mode of vibration under water, and with this added mass in air, were also determined. Finally dynamic tests of the models were made under water, and then in air with the predetermined added mass attached. Typical results obtained with the flat plate model in water and in air are shown in Fig. 6.

Results of Test Series II are summarized in Tables III and IV. Basic vibration data (periods of vibration and damping ratios) observed for the various test cases are presented in Table III together with the added mass coefficient determined for each model form. In evaluating the added mass of the water associated with the underwater vibration frequencies, it was necessary to distinguish between the water actually enclosed within the tubular form models, and the external water caused to circulate about the model. The weight added to give the same period of vibration in air represented both components, and it was necessary to subtract the weight of the water enclosed to obtain the true added mass effect. It will be noted that the added mass coefficients obtained from these free vibration studies of flexible models are significantly less than were obtained from similar studies of the rigid models.

Table IV presents the maximum bending moments resulting from the standard earthquake measured at each gage position in each model both under water, and in air with the appropriate added weights. Also presented for comparison are the theoretical maximum moments at the same locations associated with the first and second modes of vibration. These theoretical values were obtained using maximum modal accelerations taken from the experimental spectral response curves of Fig. 8 for the appropriate modal periods of vibration. In order to carry out this analysis, curves were first drawn representing the moment diagrams which would result in the first two modes of vibration from a unit modal acceleration. These curves were derived by first evaluating the maximum inertia force distribution, w(x), for the first two modes of vibration, and then integrating each twice. The maximum distributed inertia force for the nth mode of vibration is given by

$$w_n(x) = \frac{E_n}{M_n} S_{a_n} \phi_n(x) \mu(x) \qquad (4)$$

in which Sa_n = Spectral acceleration for nth mode period

$\mu(x)$ = Mass per unit length

$\phi_n(x)$ = Shape function for nth mode

$$E_n = \int_0^L \mu(x)\, \phi_n(x)\, dx$$

$$M_n = \int_0^L \mu(x)\, \phi_n^2(x)\, dx$$

The maximum bending moment diagram $\mathcal{M}_n(x)$ is then obtained by integrating twice

$$\mathcal{M}_n(x) = \iint w_n(x)\, dx\, dx = \left[\frac{E_n g}{M_n WL}\iint \mu(x)\, \phi_n(x)\, dx\, dx\right] WL \frac{Sa_n}{g} \quad (5)$$

in which $W = g\int_0^L \mu(x)\, dx$ = total weight of beam

L = length of beam

g = acceleration of gravity

Denoting the bracketed term in Eq. 5 by the symbol $\overline{\mathcal{M}}_n(x)$, it is seen that the maximum bending moments for the nth mode may be evaluated from the equation

$$\mathcal{M}_n(x) = \overline{\mathcal{M}}_n(x)\; WL \frac{Sa_n}{g} \quad (6)$$

Now it will be noted that $\overline{\mathcal{M}}_n(x)$ is the same for any uniform cantilever beam, i.e. it is independent of the total weight, and may be computed from

$$\overline{\mathcal{M}}_n(x) = \frac{E_n}{M_n L^2}\iint \phi_n(x)\, dx\, dx \quad (7)$$

Values of $\phi_n(x)$ from which $\overline{\mathcal{M}}_n(x)$ was computed for each of the first two modes of vibration are listed in Reference 9. The results of this analysis are presented in the solid lines of Fig. 9. Using these curves, the maximum moment for either of the first two modes of vibration at any point (x) in the uniform beams can be calculated merely by multiplying by WL for that beam, and by the spectral acceleration value for the appropriate period of vibration, as indicated by Eq. 6.

For non-uniform beams, it is necessary to derive $\overline{\mathcal{M}}_n(x)$ for each given weight distribution, using its definition as contained in brackets in Eq. 5. For the model beam with the mass mounted at the top, the curves representing $\overline{\mathcal{M}}_n(x)$ for the first two modes of vibration are presented by the dashed lines of Fig. 9. Using these curves, maximum moments in the first two modes of vibration for this case were also computed by means of Eq. 6.

DISCUSSION AND CONCLUSIONS

Test Series I

The principal results obtained in the first test series were the values of the added mass coefficients to be used in studying the response of rigid bodies under water. For a rigid circular section of infinite length, hydrodynamic theory gives a value of unity for the added mass coefficient, i.e. the added mass is equal to the weight of water displaced by the model. The results in Table I show rather good agreement with theory for this type of condition.

For the non-circular sections, an added mass coefficient of unity would represent a semi-circular cylinder of water attached to each face of the model in the directions facing the motion. The experimentally determined results indicate that a significantly larger volume of water than this should be assumed to move with the model. Theoretical results, as reported in Reference 6, confirm the fact that the added mass coefficient should exceed unity for a flat plate model; however, the value of 1.05 given by theory is considerably below the results observed in this study for a flat plate. It is suggested by the authors of Reference 6 that it may be difficult to achieve the experimental conditions necessary to obtain the theoretical values of the added mass coefficients for non-circular sections, and the results obtained here tend to support this suggestion. However, it also appears that the same factors might make it difficult to achieve theoretical conditions in the prototype, and it is believed that the experimental values reported herein could be applied in practice with some confidence.

The results listed in Table I show that the added mass values obtained by free vibration studies were consistently lower than the values obtained from the earthquake tests, by several percent. No explanation is offered for this discrepancy, but it is believed that the difference is small enough to ignore, and to justify the use of coefficients obtained in free vibration studies for analysis of earthquake response.

The damping ratios indicated in Table II demonstrate that the energy absorbed by internal friction of the water surrounding the models is very small, and under conditions such as those of the first test series (wherein the models were submerged deeply enough to avoid surface waves) the damping effects of the water are quite negligible.

The acceleration response spectrum presented in Fig. 8 shows generally good agreement with the response spectrum obtained by digital computer analysis of the table accelerations, probably as good as could be expected considering the accuracy with which the table accelerations could be evaluated from the oscillograph record. There is no suggestion in the experimental data of a second peak in the response spectrum in the low period range; however, the range of models tested did not extend into this range very far. The difference between results obtained for models tested in air and in water appears to imply a larger damping value under water than was measured in the free vibration tests, but data are too few to determine whether there is any significance to this trend.

<u>Test Series II</u>

The principal result to be noted from the second test series is the reduction of added mass coefficient obtained where a flexible vertical model replaced the rigid horizontal model. This reduction might be attributed to two causes. First, a flexible model will set up three-dimensional flow patterns in the water (i.e. some flow components will be directed parallel with the axis) rather than the purely two-dimensional flow associated with the rigid models. This condition has been studied by naval architects in connection with ship vibration problems (1), and is accounted for in their practice by a reduction factor depending upon the relative flexibility of the system. For some cases, reductions due to this cause may be as great as 30%. The other factor which may have contributed to the reduction of added mass coefficients in the vertical models was the fact that the models extended very close to the surface of the tank, and therefore generated surface waves when subjected to vibrations. It is difficult to evaluate the influence of this effect on the added mass coefficients, but that it is a significant factor is demonstrated by the relatively high damping values observed for the vertical models under water. The large energy losses observed here represent the effect of energy radiated off through surface waves. In any case, both of these factors can be expected in prototype earthquake conditions, and the added mass coefficients observed in these tests may be considered realistic. However, it is obvious that much remains to be learned about added mass coefficients for flexible prismatic members, and an extensive program of experimental studies along these lines is currently being initiated.

Agreement between theoretical and experimental values of bending moments obtained in the vertical models is satisfactory with respect to orders of magnitude, and this is probably all that could be expected from theoretical results obtained as they were in this analysis. It is quite clear that more than two modes would have to be considered to obtain the complete theoretical response because the second mode results generally are as significant as the first. Moreover, the actual maximum cannot be obtained by merely superposing spectral values for the two modes because of the fact that the spectral values generally do not occur at the same instant of time.

ACKNOWLEDGMENT

Adaptation of the shaking table and a preliminary investigation of rigid models was carried out by Travis Smith as a graduate research project under the direction of the writer. Design of the models for Test Series II and actual performance of all of the tests reported herein was the work of another student, Donald Brusco. The analysis of the acceleration spectrum for the table motion was carried out at the University Computer Center, using an IBM 701 Computer program prepared by Professor J. Penzien. The writer sincerely appreciates the cooperation of all these persons in carrying the work to its present status.

BIBLIOGRAPHY

1. Lewis, F. M., "The Inertia of Water Surrounding a Vibrating Ship," Transactions, Society of Naval Architects and Marine Engineers, Vol. 37, 1929.

2. Wiegel, R. L., Beebe, K. E., and Moon, J., "Ocean Wave Forces on Circular Cylindrical Piles," Proc. ASCE, Vol. 83, No. HY-2, April 1957.

3. Westergaard, H. M., "Water Pressures on Dams During Earthquakes," Trans. ASCE, Vol. 98, 1933, pp 418-434.

4. Savage, J. L., "Earthquake Investigations for the Pit River Bridge," Civil Engineering, Vol. 9, 1939, p. 470.

5. Milne-Thompson, "Theoretical Hydrodynamics," Second Edition, The Mac-Millan Company, New York, 1950.

6. Stelson, T. E. and Mavis, F. T., "Virtual Mass and Acceleration in Fluids," Trans. ASCE, Vol. 122, 1957.

7. McNown, J. S. and Keulegan, G. H., "Vortex Formation and Resistance in Periodic Motion," Proc. ASCE, Vol. 85, No. EM1, January 1959.

8. Clough, R. W. and Pirtz, D., "Earthquake Effects on Rock-Fill Dams," Trans. ASCE, Vol. 123, 1958, p. 792.

9. Young, D. and Felgar, R. P., "Tables of Characteristic Functions Representing Normal Modes of Vibration of a Beam," University of Texas, Engineering Research Series No. 44, July 1, 1949.

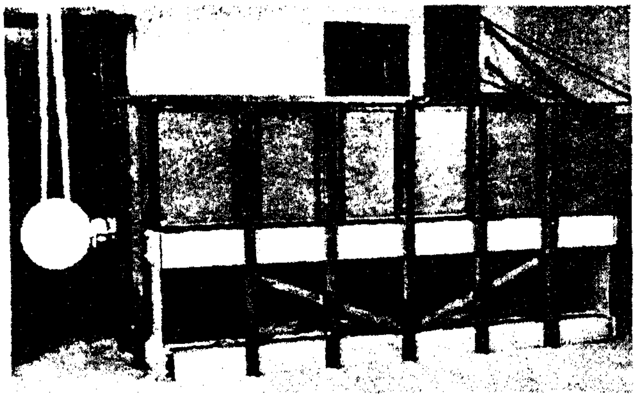

Fig. 1.
Shaking Table with Water Tank

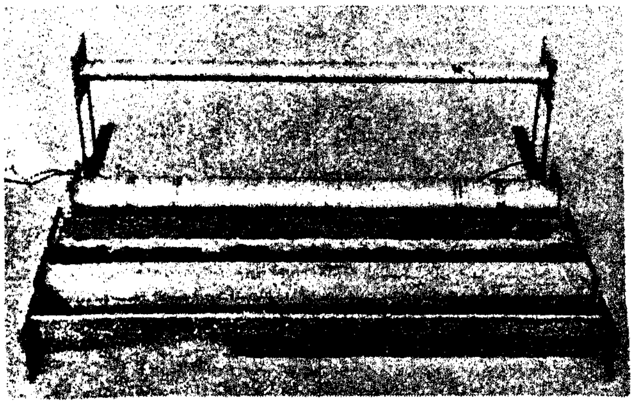

Fig. 2.
Rigid Horizontal Models; Series I

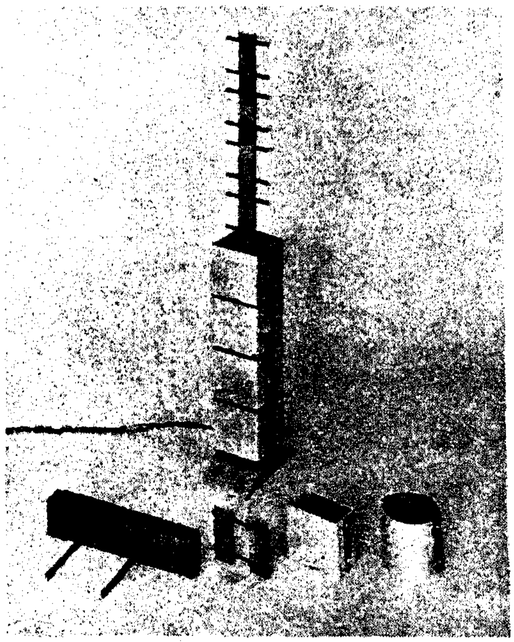

Fig. 3.
Flexible Vertical Model partially assembled, and Typical Segments; Series II

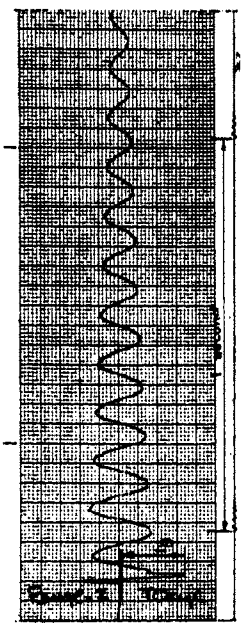

Fig. 4. "Standard" Shaking Table Accelerations

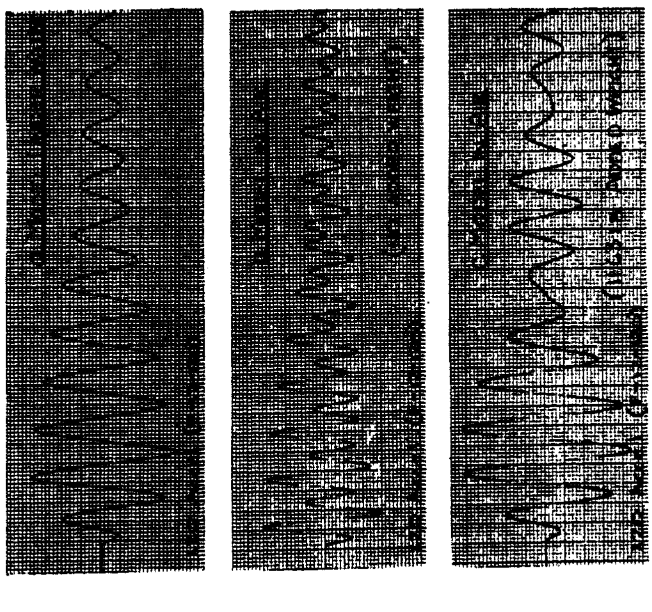

Fig. 5. Acceleration Response of 3 in. by 3 in. Model, Series I

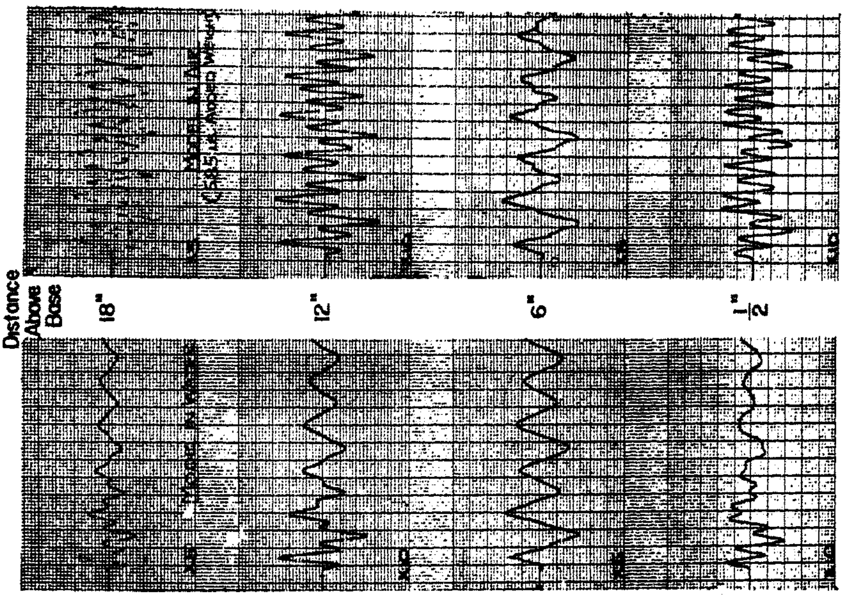

Fig. 6. Bending Moments in Flat Plate Model (in water and air), Series II

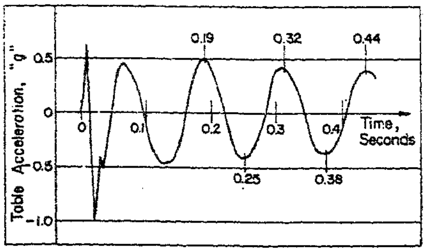

Fig. 7a. Table Accelerations during early phases of motion

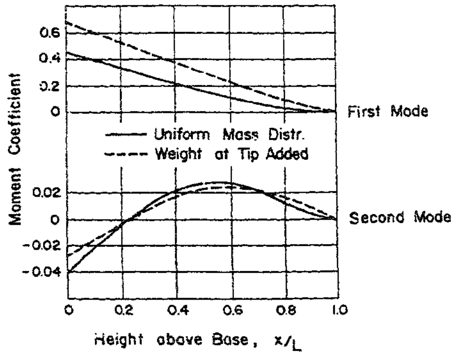

Fig. 9. Moment Influence Lines for Vertical Models, Series II

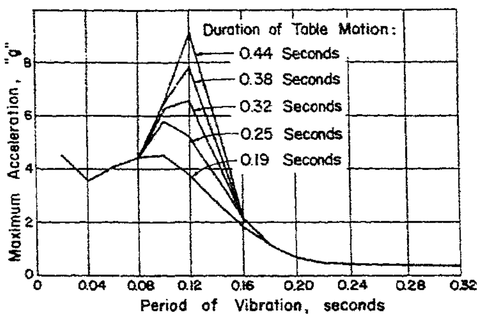

Fig. 7b. Undamped Acceleration Response Spectra for Varying Durations of Table Motion

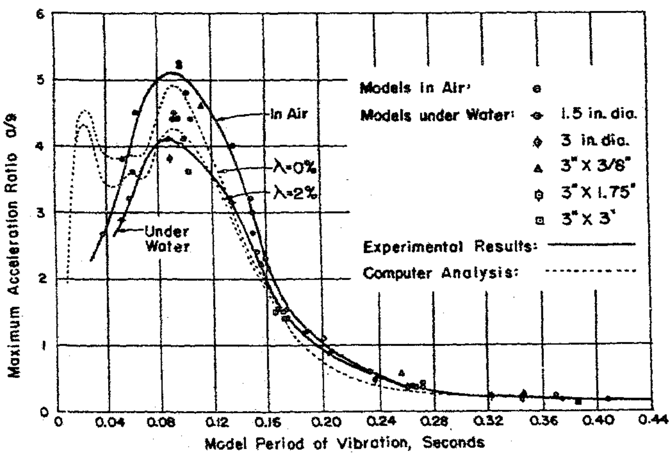

Fig. 8. Experimentally Determined Acceleration Response Spectrum

TABLE I ADDED MASS VALUES - TEST SERIES I

Model	Actual Weight (lbs)	Added Weight (lbs)		Added Mass Coefficient*	
		Earthquake Test	Free Vibrations	Earthquake Test	Free Vibrations
1 1/2 in. Dia.	1.95	2.29	2.2	1.00	0.96
3 in. Dia.	4.82	8.95	8.7	0.97	0.95
3 in x 3 in	5.87	11.63	11.2	1.26	1.22
3 in x 1 3/4 in	4.87	11.64	10.8	1.26	1.17
3 in x 3/8 in	4.95	12.21	11.6	1.33	1.26

* These represent the ratio of the added weight to the weight of water displaced by a right circular cylinder with a diameter equal to the maximum transverse dimension of the model.

TABLE II DAMPING RATIOS FROM FREE VIBRATIONS - TEST SERIES I

Model	In Air	Under Water
1 1/2 in. Dia.	0.4%	1.0%
3 in. Dia.	0.3%	0.6%
3 in x 3 in	0.4%	0.6%
3 in x 1 3/4 in	0.3%	0.8%
3 in x 3/8 in	0.4%	0.8%

TABLE III VIBRATION DATA FOR VERTICAL MODELS - TEST SERIES II

Model	Test Condition	Vibration Periods (secs)		Damping Ratios		Added Mass
		1st Mode	2nd Mode	1st Mode	2nd Mode	Coefficient
3 in. Dia.	under water	0.333	0.051	1.6%	4.5%	0.58
	in air	0.331	0.052	0.2%	2.2%	
3 in. x 3 in.	under water	0.379	0.061	2.2%	3.5%	0.82
	in air	0.380	0.059	0.2%	0.3%	
3 in. x 1 3/4 in.	under water	0.342	0.055	1.6%	2.5%	0.94
	in air	0.342	0.053	0.1%	0.6%	
3 in. x 1/4 in.	under water	0.259	0.041	4.2%	4.4%	0.95
	in air	0.261	0.042	0.2%	0.6%	
3 in. x 1/4 in.	under water	0.562	0.065	6.7%	2.6%	0.95
(with weight at top)	in air	0.562	0.064	0.5%	0.9%	

TABLE IV MAXIMUM MOMENTS IN VERTICAL MODELS - TEST SERIES II

Model	Station (inches above) base	Maximum Moment (in-lbs)			
		Under Water	With Weights in air	Theory-1st Mode	Theory-2nd Mode
3 in. Dia.	18	20	23	3	15
	12	41	40	11	26
	6	45	30	21	5
	1/2	107	98	31	32
3 in. x 3 in.	18	24	31	3	21
	12	48	49	10	37
	6	27	30	19	7
	1/2	92	98	28	46
3 in. x 1 3/4 in.	18	19	25	3	16
	12	41	41	10	28
	6	30	26	19	5
	1/2	86	86	28	35
3 in. x 1/4 in.	18	11	18	4	8
	12	29	35	12	14
	6	30	29	23	3
	1/2	56	63	33	18
3 in. x 1/4 in. (with weight at top)	18	35	35	6	24
	12	36	36	14	31
	6	12	13	23	4
	1/2	63	75	31	32